

Supplementary Information

Therapeutic Nanoworms: Towards Novel Synthetic Dendritic Cells for Immunotherapy

Subhra Mandal^{§,1}, Zaskia H. Eksteen-Akeroyd^{§,2}, Monique J. Jacobs², Roel Hammink²,
Matthieu Koepf^{2,3}, Annechien J. A. Lambeck^{1,4}, Jan C. M. van Hest⁵, Christopher J.
Wilson², Kerstin Blank^{2,*}, Carl G. Figdor^{1,*}, Alan E. Rowan^{2,*}

¹Radboud University Nijmegen, Nijmegen Centre for Molecular Life Sciences,
Department of Tumour Immunology, Geert Grooteplein 26, 6525 GA Nijmegen, The
Netherlands

²Radboud University Nijmegen, Institute for Molecules and Materials, Department of
Molecular Materials, 6525 AJ Nijmegen, The Netherlands

³present address: Energy Sciences Institute, Yale University, 300 Heffernan Drive, West
Haven, CT 06516, USA

⁴present address: University of Groningen, University Medical Center Groningen,
Department of Laboratory Medicine, Transplantation & Clinical Immunology,
Groningen, The Netherlands

⁵Radboud University Nijmegen, Institute for Molecules and Materials, Department of
Bio-Organic Chemistry, 6525 AJ Nijmegen, The Netherlands

* corresponding authors:

Dr. Kerstin Blank: k.blank@science.ru.nl; Prof. Carl G. Figdor: C.Figdor@ncmls.ru.nl; Prof. Alan E.
Rowan: a.rowan@science.ru.nl

§ authors contributed equally

Content

1. Materials	3
2. Monomer synthesis.....	3
2.1. Synthesis of the azide-functionalized isocyanide monomer (1).....	3
2.2. Synthesis of the methoxy-functionalized isocyanide monomer (2)	10
3. Polymer synthesis (3)	13
4. Polymer characterization	13
4.1. Viscosity measurements	14
4.2. Size exclusion chromatography.....	15
4.3. AFM measurements.....	16
5. Synthesis and characterization of the SA _v -polymer bioconjugate (6).....	16
5.1. Functionalization of Streptavidin with BCN-NHS (5).....	16
5.2. Synthesis of the SA _v -polymer conjugate (6).....	18
5.3. Characterization of the SA _v -polymer conjugate	18
6. Synthesis and characterization of αCD3-sDCs	19
7. Cell preparation and cell culture.....	20
8. Cell viability measurements	21
8.1. MTT assay	21
8.2. Trypan Blue assay	21
9. T cell activation	22
9.1. Flow cytometry (CD69 expression)	22
9.2. Enzyme-linked immunosorbent assay (ELISA; IFN _γ secretion)	22
9.3 Summary of all controls for CD69 expression and IFN _γ secretion.....	23
9.4. CFSE assay	24
10. Statistical analysis	25
11. Confocal imaging	26
12. Comparison of αCD3-sDC efficacy with αCD3-PLGA particles	27
11.1. Synthesis of αCD3-PLGA particles	27
11.2. Characterization of αCD3-PLGA particles	27
11.3. Estimation of the contact area and the number of possible interactions	28

1. Materials

Unless otherwise stated, all chemicals were obtained from Sigma Aldrich (Zwijndrecht, The Netherlands) and used without further purification. Toluene was distilled over sodium. Dichloromethane was distilled over phosphorous pentoxide. Column chromatography was performed using silica gel (0.060 - 0.200 mm) provided by Baker (Deventer, The Netherlands). Thin layer chromatography (TLC) analyses were carried out on silica 60 F254 coated glass obtained from Merck Millipore (Schiphol-Rijk, The Netherlands). The compounds were visualized using Ninhydrin or basic aqueous KMnO_4 solutions.

^1H NMR and ^{13}C NMR spectra were recorded on a Bruker AC-300 MHz instrument (Delft, The Netherlands) operating at 300 MHz and 75 MHz, respectively. J values are given in Hz and chemical shifts are reported in ppm. Me_4Si was used as the internal standard. FT-infrared spectra of the compounds were measured using a Thermo Nicolet IR300 FT-IR spectrometer (Thermo Fisher Scientific, Breda, The Netherlands) equipped with a Harrick ATR unit. UV/VIS measurements were done using a Varian Cary 50 spectrometer (Agilent Technologies, Amstelveen, The Netherlands). For mass spectrometry a LCQ Advantage MAX instrument (Thermo Fisher Scientific) was used.

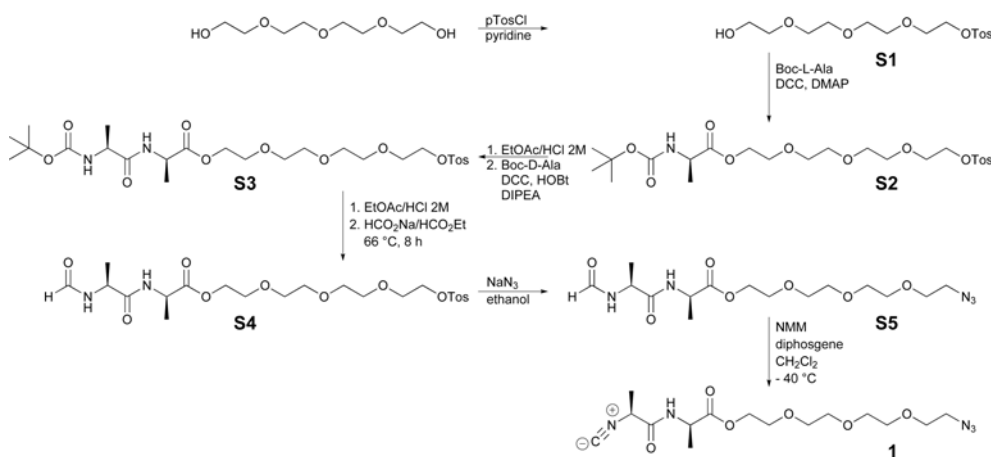
2. Monomer synthesis

2.1. Synthesis of the azide-functionalized isocyanide monomer (1)

The synthesis of (R)-2-(2-(2-(2-azidoethoxy)ethoxy)ethoxy)ethyl 2-((S)-2-isocyano propanamido)propanoate (**1**) was performed as shown in scheme S1 and is described below.

Tetraethylene glycol was tosylated to yield **S1**. Compound **S1** was then coupled to Boc-(L)-alanine *via* a carbodiimide coupling using N,N' -dicyclohexylcarbodiimide (DCC) in

the presence of 0.1 mol equivalents of 4-dimethylaminopyridine (DMAP) resulting in **S2**. The Boc group was removed using a HCl saturated ethyl acetate solution. Deprotection was monitored by TLC (SiO₂, 10 % MeOH/CH₂Cl₂).



Scheme S1. Synthetic route towards the azide-functionalized monomer (**1**)

The deprotected ethylene glycol functionalized amino acid was treated with *N,N*-Diisopropylethylamine (DIPEA) before being coupled to Boc-(*D*)-alanine *via* a DCC coupling in the presence of *N*-Hydroxybenzotriazole (HOBt) yielding **S3**. Again, the Boc protecting group of **S3** was removed using a HCl saturated ethyl acetate solution. Formamide **S4** was obtained by refluxing with 4 eq of sodium formate using ethyl formate as the solvent. Nucleophilic substitution of the tosyl-group with sodium azide resulted in **S5**. Finally, compound **S5** was dehydrated using diphosgene to obtain the isocyanide **1**.

2.1.1. Synthesis of 2-(2-(2-(2-hydroxyethoxy)ethoxy)ethoxy)ethyl 4-methylbenzene sulfonate (**S1**)

Tetraethylene glycol (28.5 mL, 164.3 mmol) was dissolved in 50 mL pyridine. The solution was subsequently cooled to 0° C while stirring. Argon was bubbled through the solution for 15 minutes. Tosylchloride (21.93 g, 115 mmol) was added portion wise to the stirring solution. The mixture was further stirred at room temperature for 12 hours.

The reaction mixture was diluted with 50 mL of 10 % citric acid. The mixture was extracted three times into 250 mL of chloroform. The combined organic layers were dried over anhydrous Na₂SO₄, filtered and evaporated under vacuum. The resulting yellow oil was purified using column chromatography (SiO₂, 0.060 - 0.200 mm; ethyl acetate as eluent) to yield **S1** as a pale yellow oil (11.69 g, 33.6 mmol, 29 %); R_f = 0.4 (ethyl acetate).

FT-IR (cm⁻¹, ATR) 3442 (O-H), 2870 (C-H), 1597 (N-H), 1453 (C-H), 1352 (S=O), 1175 (S=O), 1096 (C-O); **¹H NMR δ_H(300 MHz; CDCl₃; Me₄Si)** 7.80 (dd, J = 7.81 Hz, 2H, -CH_{Ar}-), 7.33 (d, J = 7.35 Hz, 2H, -CH_{Ar}-S), 4.17 (m, 2H, O-CH₂-CH₂-), 3.65 (m, 16H, -CH₂-), 2.45 (s, 3H, -CH₃); **¹³C NMR δ_C(75 MHz; CDCl₃; Me₄Si)** 21.16 (1C, CCH₃), 61.0 (1C, COH), 68.13(1C, COS), 69.0 (1C, OCH₂), 70.0, 70.1, 70.1, 70.2 (4C, OCH₂), 70.8, 72.0 (2C, OCH₂), 127.5 (2C, CHCCH), 129.5 (2C, CHCCH), 139.7 (1C, CCH₃), 144.5 (1C, CHCS).

2.1.2. Synthesis of (R)-2-(2-(2-(2-(tosyloxy)ethoxy)ethoxy)ethoxy)ethyl 2-((tert-butoxycarbonyl)amino)propanoate (S2)

Compound **S1** (5.23 g, 15.01 mmol), *N*-Boc-(*L*)-alanine (2.86 g, 15.01 mmol) and DMAP (0.198 g, 1.65 mmol) were dissolved in 25 mL of freshly distilled CH₂Cl₂ and cooled to 0° C while stirring. DCC (3.12 g, 15.01 mmol) was added portion wise. The mixture turned yellow and was stirred for 1 h at 0° C followed by stirring for 3 h at room temperature. The precipitated dicyclohexyl urea was removed by filtration and washed with ethyl acetate (3 x 20 mL). The organic layer was concentrated under vacuum. The crude product was purified using column chromatography (SiO₂, 0.060 - 0.200 mm; 1 % MeOH/CH₂Cl₂ as eluent) to yield **S2** as a light orange oil (5.49 g, 11.4 mmol, 76 %); R_f = 0.4 (10 % MeOH/CH₂Cl₂).

FT-IR (cm^{-1} , **ATR**) 2924 (C-H), 1745 (C=O ester), 1712 (C=O amide), 1597 (N-H), 1452 (C-H), 1352 (S=O), 1173 (S=O), 1120 (C-O); **^1H NMR** δ_{H} (**300 MHz; CDCl_3 ; Me_4Si**) 7.79 (d, $J = 8.4$ Hz, 2H, $-\text{CH}_{\text{Ar}}-$), 7.33 (d, $J = 8.1$ Hz, 2H, $-\text{CH}_{\text{Ar}}-$), 5.02 (s, 1H, $-\text{NH}-$), 4.28 (m, 3H, $-\text{CH}(\text{CH}_3)-$, COOCH_2-), 4.15 (m, 2H, $\text{O}-\text{CH}_2-\text{CH}_2-$), 3.69 (m, 14H, $\text{O}-\text{CH}_2-\text{CH}_2-$), 2.44 (s, 3H, $-\text{CH}_3$), 1.44 (s, 9H, $-\text{OC}(\text{CH}_3)_3$), 1.37 (d, $J = 7.2$ Hz, 3H, $-\text{CH}(\text{CH}_3)-$); **^{13}C NMR** δ_{C} (**75 MHz; CDCl_3 ; Me_4Si**) 18.8 (1C, CHCH_3), 21.7 (1C, CCH_3), 28.4 (3C, $\text{C}(\text{CH}_3)_3$), 49.4 (1C, $\text{O}(\text{C}=\text{O})\text{CHNH}$), 64.5 (1C, $\text{Boc}-\text{OCH}_2$), 68.9 (2C, OCH_2), 69.4 (1C, OCH_2), 70.7 (4C, OCH_2), 80.3 (1C, $\text{C}(\text{CH}_3)_3$), 128.2 (2C, CHCCH), 130.0 (2C, CHCCH), 145.0 (1C, CCH_3), 155.4 (1C, CHCS), 173.6 (1C, $\text{CH}(\text{C}=\text{O})\text{NH}$), 176.7 (1C, $\text{CH}(\text{C}=\text{O})\text{O}$); **MS (ESI) m/z $[\text{M}+\text{Na}]^+$** calcd 542.2; found 542.2.

2.1.3. Synthesis of (R)-2-(2-(2-(2-(tosyloxy)ethoxy)ethoxy)ethoxy)ethyl 2-((S)-2-((tert-butoxycarbonyl)amino)propanamido)propanoate (S3)

Compound **S2** (5.94 g, 11.4 mmol) was dissolved in 60 mL of HCl saturated ethyl acetate and stirred for 2 h at room temperature. The solvent was evaporated under vacuum and the excess of HCl was removed by adding 30 mL of CH_2Cl_2 and 1 mL of *n*-BuOH followed by evaporation. The residual *n*-BuOH was removed *via* azeotropic distillation with 3x 30 mL CH_2Cl_2 . The resulting HCl salt of **S2**, *N*-Boc-(*D*)-alanine (2.14 g, 11.4 mmol) and *N*-hydroxybenzotriazole monohydrate (HOBt; 1.74 g, 11.4 mmol) were dissolved in 40 mL freshly distilled CH_2Cl_2 . DIPEA (2 mL, 11.4 mmol) was added drop wise and the mixture was stirred at room temperature until everything was dissolved. The solution was cooled to 0 °C and DCC (2.35 g, 11.4 mmol) was added portion wise. A white precipitate was formed and the mixture was stirred for 1 h at 0° C followed by 3 h of stirring at room temperature. The precipitate was filtered off, washed with ethyl acetate (3x 30 mL) and the solvent was

evaporated under vacuum. The crude product was purified using column chromatography (SiO₂, 0.060 - 0.200 mm; 2 % MeOH/CH₂Cl₂ as eluent) to yield **S3** as a pale yellow oil (3.37 g, 5.7 mmol, 52 %); R_f = 0.3 (10 % MeOH/CH₂Cl₂).

FT-IR (cm⁻¹, ATR) 2876 (C-H), 1740 (C=O ester), 1718 (C=O amide), 1667 (N-H), 1522 (N-H), 1452 (C-H), 1365 (S=O), 1161 (S=O), 1105 (C-O); **¹H NMR δ_H(300 MHz; CDCl₃; Me₄Si)** 7.80 (d, J = 8.4, 2H, -CH_{Ar}- C-S), 7.36 (d, J = 8.1, 2H, -CH_{Ar}-), 6.91 (s, 1H, -NH), 5.00 (s, 1H, -NH), 4.58 (m, 1H, -NHCH(CH₃-)), 4.28 (m, 2H, -COOCH₂-), 4.14 (m, 2H, O-CH₂-CH₂-), 3.61 (m, 12H, -C(O)OCH₂CH₂O(CH₂CH₂O)₃-), 2.45 (s, 3H, -CH₃), 1.45 (s, 9H, -OC(CH₃)₃), 1.40 (d, J = 7.2, 3H, -CH(CH₃-)), 1.35 (d, J = 7.2, 3H, -CH(CH₃-)); **¹³C NMR δ_C(75 MHz; CDCl₃; Me₄Si)** 18.2 (2C, CHCH₃), 21.7 (1C, CCH₃), 28.4 (3C, C(CH₃)₃), 47.2 (1C, NCH), 50.0 (1C, NCH), 64.5 (1C, Boc-OCH₂), 68.7 (2C, OCH₂), 69.3 (1C, OCH₂), 70.6 (4C, OCH₂), 80.2 (1C, C(CH₃)₃), 128.0 (2C, CHCCH), 129.9 (2C, CHCCH), 133.1 (1C CCH₃), 144.9 (1C, CHCS), 172.7 (2C, C=O); **MS (ESI) m/z [M+Na]⁺** calcd 613.2; found 613.1.

2.1.4. Synthesis of (R)-2-(2-(2-(2-(tosyloxy)ethoxy)ethoxy)ethoxy)ethyl 2-((S)-2-formamidopropanamido)propanoate (S4)

Compound **S3** (1.70 g, 2.85 mmol) was deprotected following the same procedure as described for compound **S2** and used without further purification. The crude product was dissolved in 25 mL ethyl formate. Sodium formate (0.97 g, 14.25 mmol) was added and the mixture was heated for 8 hours at 66 °C. The mixture was cooled to room temperature and the solid was filtered off. The solvent was evaporated under vacuum. The crude product was purified using column chromatography (SiO₂, 0.060 - 0.200 mm; 4 % MeOH/CH₂Cl₂ as eluent) to yield **S4** as a light yellow oil (0.79 g, 1.52 mmol, 54 %); R_f = 0.3 (10 % MeOH/CH₂Cl₂).

FT-IR (cm^{-1} , **ATR**) 2873 (C-H), 1738 (C=O), 1653 (N-H), 1532 (N-H), 1452 (C-H), 1352 (S=O), 1174 (S=O), 1097 (C-O); **^1H NMR** δ_{H} (**300 MHz; CDCl_3 ; Me_4Si**) 8.18 (s, 1H, $\underline{\text{H}}\text{C}(\text{O})\text{NH}$ -), 7.79 (d, $J = 8.4$, 2H, $-\underline{\text{C}}\text{H}_{\text{Ar}}-\text{C}-\text{S}$), 7.35 (d, $J = 8.7$, 2H, $-\underline{\text{C}}\text{H}_{\text{Ar}}-$), 6.78 (s, 1H, $-\underline{\text{N}}\text{H}$), 6.55 (s, 1H, $-\underline{\text{N}}\text{H}$), 4.55 (m, 2H, $-\text{NH}\underline{\text{C}}\text{H}(\text{CH}_3)-$), 4.30 (m, 2H, $-\text{COO}\underline{\text{C}}\text{H}_2-$), 4.13 (m, 2H, $\text{O}-\underline{\text{C}}\text{H}_2-\text{CH}_2-$), 3.61 (m, 12H, $-(\underline{\text{C}}\text{H}_2\underline{\text{C}}\text{H}_2\text{O})_3-$), 2.44 (s, 3H, $-\underline{\text{C}}\text{H}_3$), 1.42 (m, 6H, $-\text{CH}(\underline{\text{C}}\text{H}_3)-$); **^{13}C NMR** δ_{C} (**75 MHz; CDCl_3 ; Me_4Si**) 17.9 (1C, CHCH_3), 18.2 (1C, CHCH_3), 21.7 (1C, CCH_3), 47.2 (1C, $\text{O}(\text{C}=\text{O})\text{HNCH}$), 48.1 (1C, $\text{HNHC}(\text{C}=\text{O})$), 64.5 (1C, OCH_2), 68.7 (2C, OCH_2), 69.3 (1C, OCH_2), 70.6 (4C, OCH_2), 128.0 (2C, CHCCH), 129.9 (2C, CHCCH), 133.1 (1C, CCH_3), 144.9 (1C, CHCCH), 161.0 (1C, $\text{H}(\text{C}=\text{O})\text{NH}$), 172.6 (1C, $\text{CH}(\text{C}=\text{O})\text{NH}$), 173.2 (1C, $\text{CH}(\text{C}=\text{O})\text{O}$); **MS (ESI)** m/z [**$\text{M}+\text{Na}$**] $^+$ calcd 541.2; found 541.2.

2.1.5. Synthesis of (R)-2-(2-(2-(2-azidoethoxy)ethoxy)ethoxy)ethyl 2-((S)-2-formamido propanamido)propanoate (S5)

Compound **S4** (0.550 g, 1.06 mmol) was dissolved in 40 mL of absolute EtOH. Sodium azide (0.38 g, 5.9 mmol) was added and the mixture was refluxed overnight. Once cooled to room temperature, the solids were removed by filtration and the filtrate was dried under vacuum. The crude product was purified using column chromatography (SiO_2 , 0.060 - 0.200 mm; 4 % MeOH/ CH_2Cl_2 as eluent) to yield **S5** a pale orange oil (0.32 g, 0.82 mmol, 78 %); $R_f = 0.4$ (10 % MeOH/ CH_2Cl_2).

FT-IR (cm^{-1} , **ATR**) 3309 (N-H), 2875 (C-H), 2105 (N_3), 1737 (C=O), 1651 (N-H), 1529 (N-H), 1453 (C-H), 1133 (C-O); **^1H NMR** δ_{H} (**300 MHz; CDCl_3 ; Me_4Si**) 8.20 (s, 1H, $\underline{\text{H}}\text{C}(\text{O})\text{NH}$ -), 6.84 (s, 1H, $-\underline{\text{N}}\text{H}$), 6.60 (s, 1H, $-\underline{\text{N}}\text{H}$), 4.60 (m, 2H, $\text{NH}\underline{\text{C}}\text{H}(\text{CH}_3)$), 4.26 (m, 2H, $-\text{C}(\text{O})\text{O}\underline{\text{C}}\text{H}_2-$), 3.68 (m, 12H, $-(\underline{\text{C}}\text{H}_2\underline{\text{C}}\text{H}_2\text{O})_3-$), 3.40 (m, 2H, $\text{N}_3\underline{\text{C}}\text{H}_2-$), 1.42 (m, 6H, $-\text{CH}(\underline{\text{C}}\text{H}_3)-$); **^{13}C NMR** δ_{C} (**75 MHz ; CDCl_3 ; Me_4Si**) 17.9 (1C, CH_3), 18.2 (1C, CH_3), 47.4 (1C, CH_2N_3), 48.4 (1C, $\text{H}(\text{C}=\text{O})\text{HNCH}$), 50.7 (1C, $\text{HNC}(\text{CH}_3)\text{C}=\text{O}$), 69.0

(1C, CH₂CH₂O), 70.1 (1C, OCH₂CH₂), 70.6 (2C, OCH₂), 70.7 (2C, OCH₂), 161.4 (1C, H(C=O)NH), 172.7 (1C, CH(C=O)NH), 172.9 (1C, CH(C=O)O); **MS (ESI) m/z** [M+Na]⁺ calcd 412.2; found 412.2.

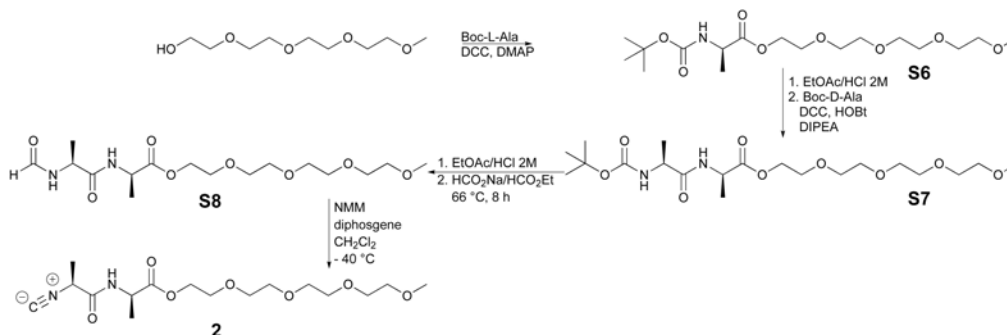
2.1.6. Synthesis of (R)-2-(2-(2-(2-azidoethoxy)ethoxy)ethoxy)ethyl 2-((S)-2-isocyanopropanamido)propanoate (1)

Compound **S5** (221 mg, 0.57 mmol) and N-methylmorpholine (NMM; 0.24 mL, 2.27 mmol) were dissolved in 150 mL freshly distilled CH₂Cl₂ and cooled down to -40 °C (dry acetone bath) under an argon atmosphere. A solution of diphosgene (0.048 mL, 0.398 mmol) in 10 mL of freshly distilled CH₂Cl₂ was added drop wise under argon over 1 h. While adding diphosgene, the mixture was stirred and kept strictly at -40 °C. Once the mixture began to turn yellow, the reaction was rapidly quenched with an excess of sodium bicarbonate (5 g). The quenched mixture was stirred for 5 minutes at -40 °C. The reaction mixture was passed over a short silica column plug (SiO₂, 0.060 - 0.200 mm). The plug was packed with CH₂Cl₂ but the desired compound was eluted with CH₂Cl₂/acetonitrile (3:1) to yield **1** as a pale yellow oil (48.1 mg, 0.48 mmol, 27 %); R_f = 0.5 (10 % MeOH/CH₂Cl₂).

FT-IR (cm⁻¹, ATR) 3318 (N-H), 2875 (C-H), 2142 (C≡N), 2105 (N₃), 1744 (C=O), 1540 (N-H), 1453 (C-H), 1123 (C-O); **¹H NMR δ_H(300 MHz; CDCl₃; Me₄Si)** 7.00 (bd, 1H, -NH-), 4.59 (m, 1H, -NHCH(CH₃)C(O)O-), 4.32 (m, 3H, (-C(O)OCH₂CH₂O-), -C≡NCH(CH₃)C(O)NH-), 3.67 (m, 12H, -(OCH₂CH₂)₃), 3.39 (m, 2H, N₃CH₂-), 1.65 (d, J = 7.2, 3H, C≡NCH(CH₃)C(O)-), 1.48 (d, J = 7.2, 3H, C≡NCH(CH₃)C(O)-); **¹³C NMR δ_C(75 MHz; CDCl₃; Me₄Si)** 170.69 (1C, CH(CH₃)C(O)OCH₂), 165.72 (1C, CH(CH₃)C(O)NH), 70.69, 70.65, 70.61, 70.56, 70.02, 68.81 (1 C, CH₂CH₂O), 50.66 (1C, CH₂N₃), 48.56 (C≡NCH), 19.66, 18.04 (1C, CH(CH₃)CO); **MS (ESI) m/z** [M+Na]⁺ (C₁₅H₂₅N₅O₆Na), calcd 394.17; found 394.1.

2.2. Synthesis of the methoxy-functionalized isocyanide monomer (compound 2)

The synthesis of (S)-2,5,8,11-tetraoxatridecan-13-yl 2-((R)-2-isocyanopropanamido)propanoate (**2**) was performed as shown in scheme S2 and has been reported previously.^{1,2}



Scheme S2. Synthetic route towards the methoxy-functionalized monomer (**2**)

Tetraethylene glycol monomethyl ether was coupled to Boc-(L)-alanine to obtain **S6** via DCC coupling in the presence of 0.1 mol equivalents of DMAP. **S6** was deprotected using a HCl saturated ethyl acetate solution. After deprotection, **S6** was coupled to Boc-(D)-alanine via a DCC coupling in the presence of HOBT. The product **S7** was again deprotected using a HCl saturated ethyl acetate solution until no more starting material could be observed by TLC analysis (SiO₂, 5 % MeOH/CH₂Cl₂). The deprotected amine was formylated with sodium formate to obtain formamide **S8**. After purification, **S8** was dehydrated with diphosgene to obtain the isocyanide **2**.

2.2.1. Synthesis of (R)-2,5,8,11-tetraoxatridecan-13-yl 2-((tert-butoxycarbonyl)amino)propanoate (**S6**)

Tetraethylene glycol monomethylether (5.01 g, 24.1 mmol), N-Boc-(L)-alanine (4.47 g, 23.6 mmol) and DMAP (0.37 g, 3.0 mmol) were dissolved in 30 mL of freshly distilled CH₂Cl₂ and cooled to 0 °C while stirring. DCC (4.96 g, 24.0 mmol) was added and the mixture turned yellow gradually. It was stirred for 1 h at 0 °C and allowed to heat up to room temperature for another 3 h. The precipitate was filtered off, washed with ethyl

acetate (3 x 20 mL) and the filtrate was dried under vacuum. The crude product was purified using column chromatography (SiO₂, 0.060 - 0.200 mm; 1 % MeOH/CH₂Cl₂ as eluent) to yield **S6** as an orange oil (7.24 g, 19.08 mmol, 80.7 %); R_f = 0.8 (CH₂Cl₂).

FT-IR (cm⁻¹, ATR): 3344 (N-H), 2878 (C-H), 1757 (C=O ester), 1712 (C=O protecting group), 1520 (N-H), 1453 (C-H), 1165 (C-O); **¹H NMR δ_H(300 MHz; CDCl₃; Me₄Si)** 5.08 (s, 1H, -NH-), 4.29 (m, 3H, -CH(CH₃)-, COOCH₂-), 3.65 (m, 14H, -CH₂-), 3.38 (s, 3H, -OCH₃), 1.43 (d, J = 1.39 Hz, 9H, -C(CH₃)-), 1.37 (s, 3H, -CH(CH₃)-).

2.2.2. Synthesis of (R)-2,5,8,11-tetraoxatridecan-13-yl 2-((S)-2-((tert-butoxycarbonyl)amino)propanamido)propanoate (S7)

Compound **S7** was synthesized according to the same procedure as compound **S3**. The crude product was purified using column chromatography (SiO₂, 0.060 - 0.200 mm; 2 % MeOH/CH₂Cl₂ as eluent) to yield **S7** as a slightly yellow oil (4.43 g, 9.5 mmol, 63 %); R_f = 0.5 (10 % MeOH/CH₂Cl₂).

FT-IR (cm⁻¹, ATR) 3317 (N-H), 2876 (C-H), 1739 (C=O ester), 1671 (N-H), 1517 (N-H), 1452 (C-H), 1163 (C-O); **¹H NMR δ_H(300 MHz; CDCl₃; Me₄Si)** 6.80 (s, 1H, -NHCH-), 5.11 (bs, 1H, -NHCH), 4.60 (q, J = 8.56 Hz, 1H, -NHCH(CH₃)-), 4.28 (m, 3H, -C(O)OCH₂CH₂O-, -CH(CH₃)COO-), 3.73-3.64 (m, 14H, -C(O)OCH₂CH₂O(CH₂CH₂O)₃-), 3.39 (s, 1H, -OCH₃), 1.46 (s, 9H, -OC(CH₃)₃), 1.43 (d, J = 1.40 Hz, 3H, -NHCH(CH₃)-), 1.36 (d, J = 1.33 Hz, 3H, -NHCH(CH₃)-).

2.2.3. Synthesis of (S)-2,5,8,11-tetraoxatridecan-13-yl 2-((R)-2-formamidopropanamido)propanoate (S8)

Compound **S8** was synthesized according to the same procedure as described for compound **S4**. The crude product was purified using column chromatography (SiO₂, 0.060 - 0.200 mm; 4 % MeOH/CH₂Cl₂ as eluent) to yield **S8** as a colorless oil (1.74 g, 4.6 mmol, 69 %); R_f = 0.4 (10 % MeOH/CH₂Cl₂).

FT-IR (cm^{-1} , **ATR**) 3297 (N-H), 2875(C-H), 1739 (C=O ester), 1653 (N-H), 1529(N-H), 1452 (C-H), 1101 (C-O); **^1H NMR** δ_{H} (**300 MHz; CDCl_3 ; Me_4Si**) 8.21 (s, 1H, -C(O)NH-), 6.96 (bd, $J=7.5\text{Hz}$, 1H, -NHCH-), 6.79 (bd, $J=7.5\text{Hz}$, 1H, -NHCH-), 4.58 (m, 2H, NHCH(CH₃)), 4.31 (m, 2H, -C(O)OCH₂-), 3.67-3.56 (m, 14H, -C(O)OCH₂CH₂O(CH₂CH₂O)₃-), 3.39 (s, 3H, -OCH₃), 1.43 (m, 6H, -NHCH(CH₃)-, -NHCH(CH₃)-).

2.2.4. Synthesis of (S)-2,5,8,11-tetraoxatridecan-13-yl 2-((R)-2-isocyanopropanamido)propanoate (2)

Compound **2** was synthesized according to the same procedure as compound **1**. The crude product was purified using column chromatography (SiO_2 , 0.060 - 0.200 mm; CH_2Cl_2 /acetonitrile 3:1 as eluent) to yield **2** as a colorless oil (174 mg, 0.48 mmol, 63 %); $R_f = 0.4$ (10 % MeOH/ CH_2Cl_2).

FT-IR (cm^{-1} , **ATR**) 3250 (N-H, amide), 2875 (C-H), 2140 (C \equiv N, isocyanide), 1741 (C=O, ester), 1682 (C=O, amide), 1100 (C-O, ether); **^1H NMR** δ_{H} (**300 MHz; CDCl_3 ; Me_4Si**) 6.99 (bd, 1H, -NH-), 4.58 (m, 1H, -NHCH(CH₃)C(O)O-), 4.32 (m, 2H, -C(O)OCH₂CH₂O-), 4.25 (m, 1H, C \equiv NCH(CH₃)C(O)NH-), 3.73-3.53 (m, 14H, -OCH₂CH₂(OCH₂CH₂)₃OCH₃), 3.37 (s, 3H, -OCH₃), 1.64 (d, $J = 7.2$ Hz, 3H, C \equiv NCH(CH₃)C(O)-), 1.49 (d, $J = 7.2$ Hz, 3H, -NHCH(CH₃)C(O)O-); **^{13}C NMR** δ_{C} (**75 MHz; CDCl_3 ; Me_4Si**) 171.98 (-CH(CH₃)C(O)OCH₂-), 165.73 (-CH(CH₃)C(O)NH-), 160.9 (C \equiv N-), 71.92 (-CH₂CCH), 70.60, 70.60, 70.60, 70.51, 70.51, 68.8, 65.55 (-OCH₂CH₂O)₃-), 64.72 (-C(O)OCH₂-), 59.00 (-OCH₃), 48.58 (C \equiv NCH(CH₃)CONH-), 48.58 (-NHCH(CH₃)C(O)O-), 19.66 (C \equiv NCH(CH₃)CONH-), 18.02 (NHCH(CH₃)C(O)O-); **MS (ESI) m/z [$\text{M}+\text{Na}$]⁺** ($\text{C}_{18}\text{H}_{39}\text{N}_2\text{O}_7\text{Na}$), calcd 383.1; found 383.2.

3. Polymer synthesis (3)

Compound **1** (3.1 mg, $8.3 \cdot 10^{-3}$ mmol) and compound **2** (300 mg, $8.3 \cdot 10^{-1}$ mmol) were dissolved in 30 mL of distilled toluene yielding a ratio of azide-functionalized monomers (**1**) to methoxy-functionalized monomers (**2**) of 1:100. The catalyst stock solution was prepared separately by dissolving $\text{Ni}(\text{Cl}_2\text{O}_4)_2 \cdot 6 \text{H}_2\text{O}$ (30.7 mg, $8.4 \cdot 10^{-2}$ mmol) in 10 mL of absolute ethanol and 90 mL of toluene. From the catalyst stock solution $8.3 \cdot 10^{-5}$ mmol was added to the reaction mixture. The mixture was stirred for 3 days at room temperature (RT). The reaction was followed by IR until all isocyanide was consumed (peak at 2142 cm^{-1}). The polymer (compound **3**) was isolated *via* precipitation into diisopropylether. This precipitation cycle was repeated thrice to obtain 299.6 mg, 78 % yield.

4. Polymer characterization

The molecular weight M_w of the resulting polymer was determined from both viscosity and size exclusion chromatography (SEC) measurements. In addition, the polymer length was determined using atomic force microscopy (AFM). The corresponding experiments are described in detail below. The results are summarized in table S1.

Table S1. Summary of molecular weight M_w and polymer length l

	molecular weight M_w (kg/mol)	apparent polymer length l (nm)
\bar{M}_v viscosity	421	123 ^a
M_w SEC	588	172 ^a
AFM	677 ^b	197

^aThe apparent polymer length l was calculated from the measured molecular weight:

$$l = M_w \cdot \frac{1}{4} \cdot \frac{1}{360 \text{ g/mol}} \cdot 0.42 \text{ nm}$$

^bThe molecular weight M_w was calculated from the experimentally determined polymer

$$\text{length: } M_w = l \cdot 4 \cdot 360 \text{ g/mol} \cdot \frac{1}{0.42 \text{ nm}}$$

4.1. Viscosity measurements

The intrinsic viscosity of polymer **3** was obtained from measurements with an Ubbelohde viscometer (Schott Instruments, Mainz, Germany). A stock solution (4 mg/mL) of polymer **3** was prepared in acetonitrile. From this stock solution, 4 mL of the following concentrations were prepared: 0.6; 0.5; 0.4; 0.3; 0.2 and 0.1 mg/mL. The solutions were loaded into a viscometry tube (nr. 1053431; Schott Instruments). The tube was placed into the water bath (25 °C) and allowed to equilibrate for 15 min before the measurement. The flow speed for each sample was measured four times and used to determine the kinematic viscosity ν . From this data, the reduced viscosity η_{red} and the inherent viscosity η_{inh} were calculated³ and plotted against the polymer concentration. The intrinsic viscosity $[\eta]$ represents the limiting value of η_{red} or η_{inh} at infinite dilution of the polymer, *i.e.* $[\eta] = \lim_{c \rightarrow 0} \eta_{\text{inh}}$. From extrapolation of η_{red} to $c = 0$, an intrinsic viscosity $[\eta] = 9.64 \text{ dL} \cdot \text{g}^{-1}$ was obtained (Figure S1).

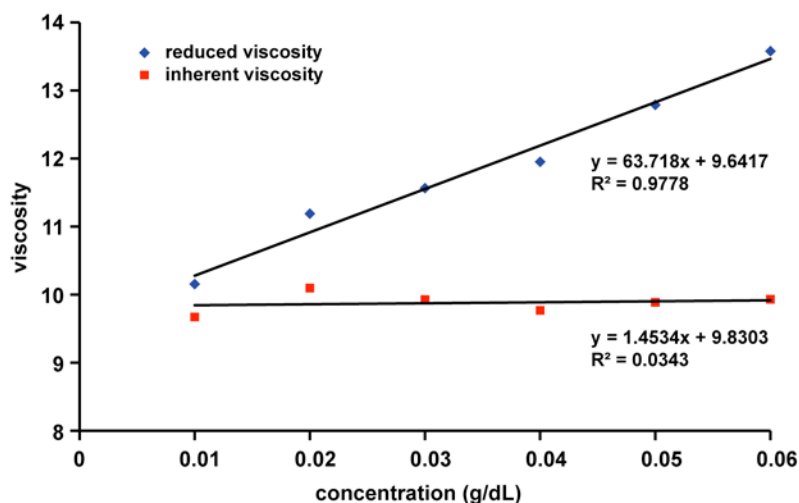


Figure S1. Ostwald viscosity measurement. The intrinsic viscosity was determined experimentally from both the reduced viscosity and the inherent viscosity for different concentrations of the polymer in acetonitrile. The value for the intrinsic viscosity $[\eta] = 9.64 \text{ dL} \cdot \text{g}^{-1}$ was obtained from extrapolation to $c = 0 \text{ g/dL}$.

Based on $[\eta]$, a molecular weight of 421 kg/mol was determined using the Mark-Houwink equation $[\eta] = K \overline{M}_v^a$. The constants $K = 1.4 \cdot 10^{-9} \text{ dL} \cdot \text{mol}^a \cdot \text{g}^{-(1+a)}$ and $a = 1.75$ for a rigid polyisocyanide have been reported previously.⁴ The average polymer length was calculated to be 123 nm (Table S1).

4.2. Size exclusion chromatography

Polymer **3** was further analyzed by size exclusion chromatography (SEC) to determine its hydrodynamic radius. The SEC system was equipped with a Waters 1515 Isocratic HPLC pump, a Waters 2414 refractive index detector, a Waters 2707 autosampler, a PSS PFG guard column followed by 2 PFG-linear-XL (7 μm , 8*300 mm) columns in series. The system was run at 40 °C. Hexafluoroisopropanol (HFIP, Biosolve) with potassium trifluoroacetate (3 g/L) was used as eluent at a flow rate of 0.8 mL/min.

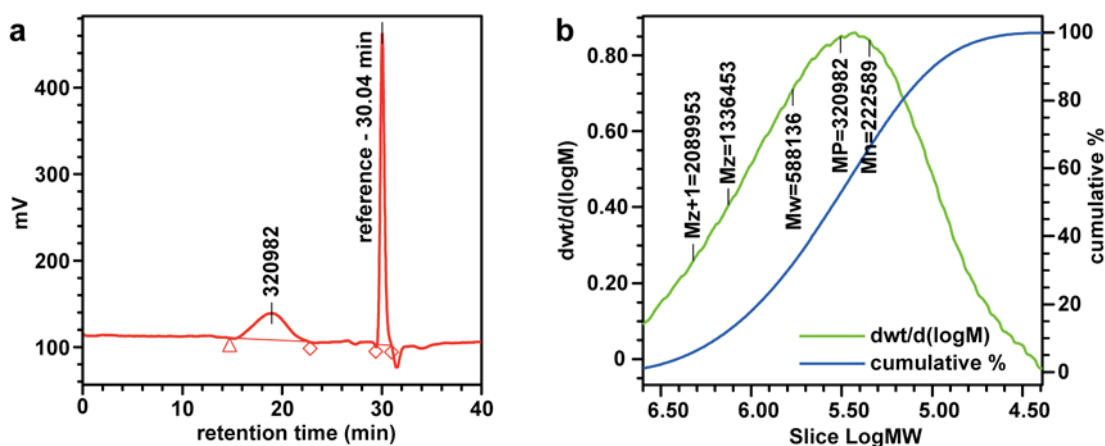


Figure S2. Size exclusion chromatography. a) Compound **3** eluted at 18.5 min. b)

This corresponds to a weighted average molecular weight M_w of 588 kg/mol (PMMA standards) and a PDI of 2.6.

The molecular weights were calculated against poly(methyl methacrylate) standards ($M_p = 580 \text{ Da}$ up to $M_p = 7.1 \cdot 10^6 \text{ Da}$; Agilent). The measurement yielded a molecular

weight of 588 kg/mol and the average polymer length was calculated to be 172 nm (Figure S2 and Table S1).

4.3. AFM measurements

The polymer sample was diluted in 1 mM sodium acetate buffer pH 4.5 to obtain a concentration between 0.5 $\mu\text{g/mL}$ and 5 $\mu\text{g/mL}$. The samples were drop casted onto freshly cleaved and polylysine coated mica and incubated for 10 minutes. The remaining liquid was removed and the sample was dried in a stream of N_2 . AFM images were recorded in tapping mode in air using a Nanoscope IV instrument (Bruker) and NSG-10 tapping mode tips (NT-MDT, Limerick, Ireland). The polymer length was determined by hand using the program ImageJ⁵ (Figure S3 and Table S1).

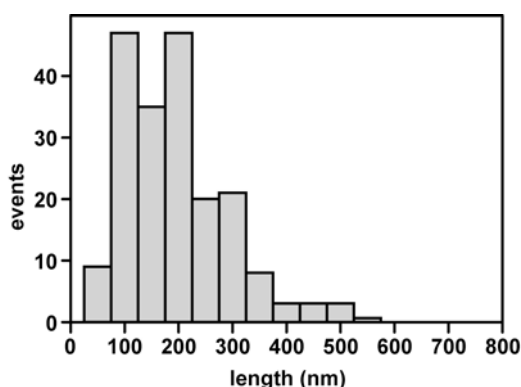


Figure S3. Measurement of the polymer length with AFM. The mean value is 197 nm ($n = 198$).

5. Synthesis and characterization of the SA_v-polymer bioconjugate (6)

5.1. Functionalization of Streptavidin with BCN-NHS (5)

Streptavidin (SA_v) was obtained from Thermo Fisher Scientific (Etten-Leur, The Netherlands) and 2,5-dioxopyrrolidin-1-yl 1-(bicyclo[6.1.0]non-4-yn-9-yl)-3,14-dioxo-2,7,10-trioxa-4,13-diazaoctadecan-18-oate (BCN-NHS; compound **4**) was obtained

from Synaffix (Nijmegen, The Netherlands). SAV (34.5 mg, $5.2 \cdot 10^{-4}$ mmol) was dissolved in 7 mL of borate buffer (10 mM, pH 8.5) and BCN-NHS (1.7 mg, $3.1 \cdot 10^{-3}$ mmol) was added to the SAV solution. The mixture was kept at 4 °C for four days. BCN-functionalized SAV (compound **5**) was purified by gel filtration (PD 10 column, GE Healthcare) followed by ultrafiltration (Amicon Ultra-4, 10 kDa; Merck Millipore). The final yield of **5** was determined by measuring absorption at 280 nm. Using an extinction coefficient of $\epsilon = 167280 \text{ mol}^{-1} \text{ cm}^{-1}$, the yield was determined to be 26.1 mg, 76 %. The conjugate was further characterized using MALDI-ToF to obtain the labeling ratio. MALDI-ToF was performed using a Bruker Biflex III MALDI-ToF spectrometer. SAV and SAV-BCN samples were prepared using α -Cyano-4-hydroxycinnamic acid as the matrix. The mass obtained for SAV (monomer) was determined to be 13280 Da [$M^+ H^+$]. This served as a reference for **5**. Compound **5** shows both the peak of the non-functionalized monomer of 13280 Da [$M^+ H^+$] as well as the mass of **5** carrying one BCN-group coupled to the SAV monomer: 13783 Da [$M^+ 2K^+$] (Figure S4). No peak corresponding to a doubly labelled monomer was visible. Consequently, the degree of functionalization is between 0 and 4 BCN-groups for the SAV tetramer.

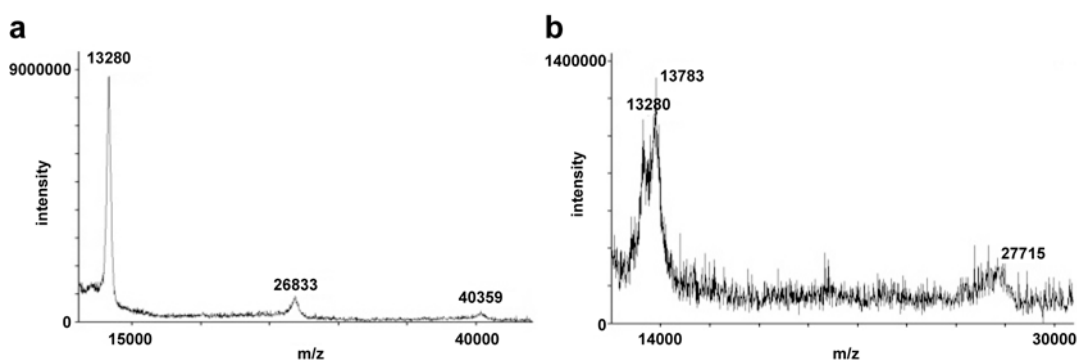


Figure S4. MALDI-ToF analysis. a) SAV before addition of BCN-NHS; b) BCN-functionalized SAV.

5.2. Synthesis of the SAV-polymer conjugate (6)

Polymer **3** in 10 mL of 10 mM borate buffer (10 mg, $2.7 \cdot 10^{-5}$ mmol) was mixed with SAV-BCN (26 mg, $3.9 \cdot 10^{-7}$ mmol) in 4 mL of 10 mM borate buffer. The mixture was incubated at 4 °C for four days to obtain polymer **6**. Polymer **6** was purified by dialysis against water at 4 °C for 2 days using a membrane with cut-off of 100 kDa.

5.3. Characterization of the SAV-polymer conjugate (6)

5.3.1. Circular dichroism measurements

To ensure that the bioconjugation does not affect the structure of the poly(isocyanopeptide) polymer, circular dichroism spectra were recorded for both polymer **3** and polymer **6**. The measurements were performed at 20 °C at a concentration of 1 mg/mL in 50 mM borate buffer pH 8.5 using a Jasco J-810 CD spectrometer (de Meern, The Netherlands). Both polymers showed identical spectra (Figure S5) clearly indicating that the coupling of SAV does not influence the secondary structure of the SAV-polymer conjugate.

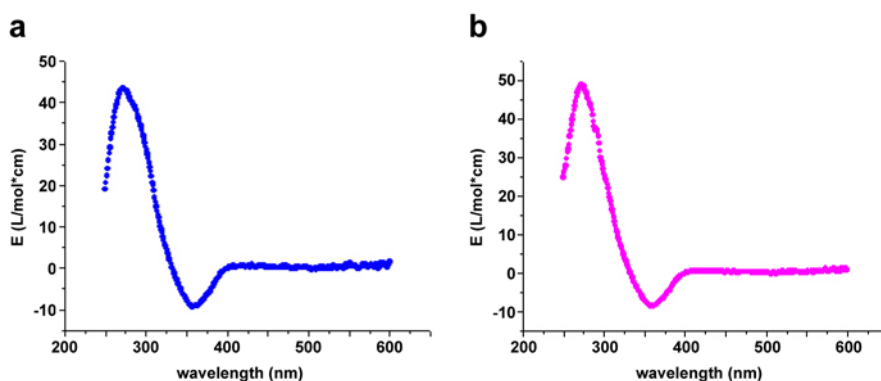


Figure S5. Circular dichroism spectra. a) polymer 3; b) SAV-polymer conjugate 6.

5.3.2. AFM measurements

The SAV loading of **6** was determined with AFM using the same procedure as for polymer **3**. The results of this analysis are shown in the main text (Figure 3).

6. Synthesis and characterization of α CD3-sDCs

To obtain the α CD3-sDCs, the α CD3 antibodies were first biotinylated with EZ-Link Sulfo-NHS-LC-Biotin (Thermo Fisher Scientific) to allow for binding to SAV on polymer **6**. Before preparing the α CD3-sDCs, the molecular ratio of α CD3:SAV bound to the sDCs was optimized using a biotinylated AlexaFluor488-labelled α CD3 antibody. Using the fluorescently labelled antibody, it was possible to determine the α CD3 concentration while measuring the total protein concentration in the same sample.

First, the SAV concentration on polymer **6** was determined using a BCA micro assay (Thermo Fisher Scientific). Then polymer **6** was mixed with the AlexaFluor488-labelled and biotinylated α CD3 antibody using 4:1, 6:1 and 8:1 molar ratios of α CD3:SAV. The mixture was left at 4 °C for 24 h. After removing the free α CD3 by ultrafiltration (Nanosep Omega, cut-off of 300 kDa, PALL Life Sciences, Zaventem, Belgium) the total protein concentration was again determined using the BCA assay. In addition, the fluorescence originating from the AlexaFluor488-labelled antibody was determined from a fluorescence measurement in a microplate reader (Cytofluor II, PerSeptive Biosystems, Framingham, MA, USA). The α CD3 concentration was calculated from a standard curve of AlexaFluor488-labelled α CD3. Subtracting the Alexa488- α CD3 concentration from the total protein concentration, the SAV concentration as well as the α CD3:SAV ratio was determined. For a 4:1 mixing ratio of α CD3:SAV approximately one α CD antibody was bound per SAV molecule (Figure S6).

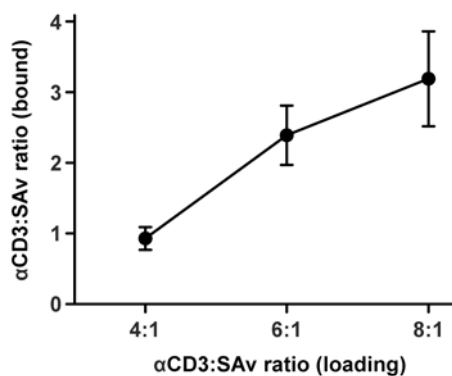


Figure S6. Loading of polymer 6 with α CD3 antibodies. Different ratios of biotinylated, AlexaFluor488-labelled α CD3 were added to polymer **6** (α CD3:SAv ratio = 4:1, 6:1 and 8:1). For a ratio of 4:1, an average number of 0.93 α CD3 molecules was obtained per SAv molecule. For 6:1 and 8:1, a final ratio of 2.69 and 3.37 α CD molecules were bound per SAv molecule, respectively. Mean values and standard deviations were determined from 8 experiments ($n = 8$).

To prepare the sDCs for the T cell experiments, a 4:1 mixing ratio was used following exactly the same protocol as used in the preliminary experiment described above. Assuming that the ratio of bound α CD3:SAv will be identical, the concentration of α CD3 could now be determined from the total protein concentration without the need for fluorescently labelling the α CD3 antibody. For the T cell experiments, all the treatment concentrations were based on the concentration of α CD3 present on the sDC backbone, on the microbead system or as free α CD3.

7. Cell preparation and cell culture

Peripheral Blood Lymphocytes (PBLs) were isolated from the buffy-coat obtained from a healthy volunteer via Ficoll density gradient centrifugation (Lucron Bioproducts, Sint Martens-Latem, Belgium). The PBLs and OKT3 hybridoma were always maintained in RPMI-1640 medium (Life Technologies, Bleiswijk, The Netherlands) containing 10 %

Fetal Bovine Serum (FBS) (Greiner Bio-One B.V., Alphen a/d Rijn, The Netherlands), 1 % glutamine (Lonza, Breda, The Netherlands) and 1x Antibiotic-Antimycotic (Life Technologies). For the α CD3 production, OKT3 hybridoma cells (at confluence) were transferred into Protein Free Hybridoma Medium (PFHM-II, Life Technologies). These cells were cultured for 3-4 days in PFHM-II before purifying the α CD3 monoclonal antibodies using HiTrap™ Protein G HP Columns (GE healthcare, Little Chalfont, UK).

8. Cell viability measurements

8.1. MTT assay

The cytotoxic effect of the α CD3-sDCs was determined using a standard MTT assay.⁶ PBLs (10^5 cells/well) were treated with α CD3-sDC, α CD3 or left untreated (control) for 24 h using different concentrations (5, 50, 500 ng/mL) of the respective molecules. After washing twice, the cells were incubated with MTT (5 mg/mL; Sigma Aldrich) for 2 h. The medium was then replaced with 100 μ l of DMSO. After solubilization, the microplates were read at 550 nm using a microplate reader (iMark, Bio-Rad, Veenendaal, The Netherlands). The results were derived from three independent experiments (with three replicates per experiment).

8.2. Trypan Blue assay

In addition, the cell viability was estimated over time. Viable and non-viable cells were counted after α CD3-sDC treatment using the hemacytometer method by means of a Trypan Blue assay.⁷ The percentage of viable cells was determined upon exposure to α CD3-sDC, α CD3, and untreated (control) in a concentration of 200 ng/mL and incubation times of 0, 24 and 72 h. The percentage of viable cells was calculated according to the formula: $100 \times (\text{number of viable cells in treated samples} / \text{total number})$

of cell counted). The results were obtained from three independent experiments (with three replicates per experiment).

9. T cell activation

9.1. Flow cytometry (CD69 expression)

The estimation of activated T cells (CD69⁺ T cells) upon α CD3-sDC treatment was determined using Fluorescence Activated Cell Scanning (FACS). Briefly, PBLs (10^5 /well) were treated with the respective molecules for 24 h at different concentrations (0.005, 0.01, 1, 5, 10, 50, 100 ng/mL). In addition to these concentration dependent experiments, also time dependent T cell activation studies were performed. The T cells were treated with α CD3-sDC and α CD3 using a concentration of 5 ng/mL and incubation times of 2, 4, 6, 8, 10, 24, 28 and 30 h. The treated cells were washed with PBS containing 10 % BSA (PBA; Sigma Aldrich). Subsequently, the cells were incubated with Fluorescein-labelled mouse anti-human CD69 mAb (activated T cell marker, BD Biosciences, Breda, The Netherlands) and APC-labelled mouse anti-human CD4/8 mAb (T cell marker, BD Biosciences). After washing twice with PBA, FACS analysis was performed using a CyAn™ ADP Analyzer instrument (Beckman Coulter, Woerden, The Netherlands). The results were analyzed using Flow-Jo ver. 9.2 software (Tree Star Inc., Ashland, OR, USA). The above experiment was repeated four independent times (with three replicates per experiment).

9.2. Enzyme-linked immunosorbent assay (ELISA; IFN γ secretion)

The level of secreted IFN γ was determined in the culture supernatants using a standard sandwich ELISA method. After coating overnight at 4 °C with mouse anti-human IFN γ antibody (Thermo Fisher Scientific), the 96-well microplates (Nunc Immunomodules;

Thermo Fisher Scientific) were washed with PBS/Tween (0.05 %) and blocked with PBS-1 % BSA. Subsequently, the IFN γ standards (Thermo Fisher Scientific) and the supernatants were added into the wells and incubated for 1 hour at room temperature. Following washing with PBA for three times, the presence of IFN γ was detected using a biotinylated mouse anti-human IFN γ antibody (Thermo Fisher Scientific) and a streptavidin-horseradish peroxidase (HRP) conjugate (Life Technologies). HRP activity was detected using tetramethyl benzidine (TMB; Sigma Aldrich). The absorption was measured at 450 nm using an iMark Microplate Reader (Bio-Rad). The experiments were conducted for four independent times.

9.3. Summary of all controls for CD69 expression and IFN γ secretion

The level of CD69 expression as well as the concentration of the secreted IFN γ was determined for α CD3-sDC and for the following controls: non-biotinylated, free α CD3 antibodies (α CD3); biotinylated α CD3 bound to streptavidin (α CD3-SAv); biotinylated α CD3 bound to streptavidin functionalized PLGA particles (see 12, α CD3-PLGA); non-biotinylated α CD3 mixed with polymer **6** (polymer **6** + α CD3); polymer **6** alone (polymer **6**); polymer **3** alone (polymer **3**); streptavidin alone (SAv); non-biotinylated, free mouse anti-human IgG_{2a} antibodies as α CD3 isotype control (mIgG_{2a}); biotinylated mIgG_{2a} antibodies bound to polymer **6** (mIgG_{2a}-sDC). The results of all treatment conditions are summarized in Figure S7.

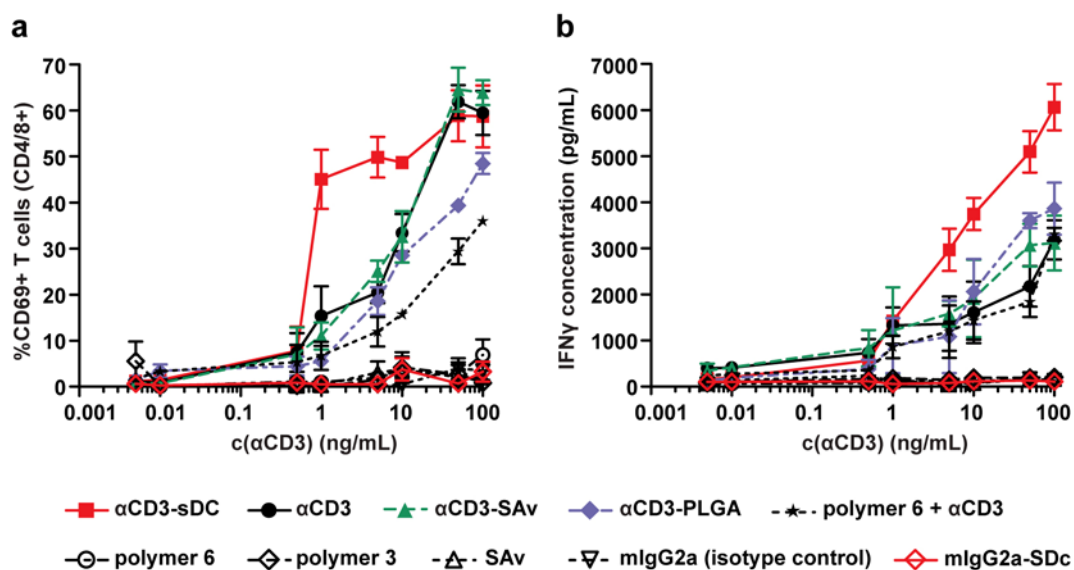


Figure S7. T cell activation profile based on the early activation marker CD69 (a) and late activation marker IFN γ (b). Each value represents the mean \pm s.e.m. of three independent donors.

9.4. CFSE assay

T cell proliferation induced by α CD3-sDC was assessed using a CFSE assay.⁸ PBLs (10^5) were pre-labelled with 5 μ M CFSE (Life Technologies). Free CFSE was quenched with FBS. α CD3-sDC and α CD3 was added to the CFSE-labelled PBLs (10^5 /well) at a concentration of 5 ng/mL. Treated cells were incubated overnight along with untreated control cells. After incubation times of 0, 24, 48, 72 and 96 h, the treated cells were used for FACS analysis. T cells were identified based on labelling with a mouse APC-labelled anti-human CD4/8 antibody. T cell proliferation was assessed from determining the CFSE staining intensity. The results were interpreted by considering the % decrease in fluorescence intensity as a corresponding % increase in T cell proliferation. The % difference in T cell proliferation (% Δ PF) was determined by normalizing the treated value against the untreated (control) value. Cyton software was utilized to analyze the

number of cells proliferated per generation⁹ (Figure S8). The results were derived from four independent experiments (with three replicates per experiment).

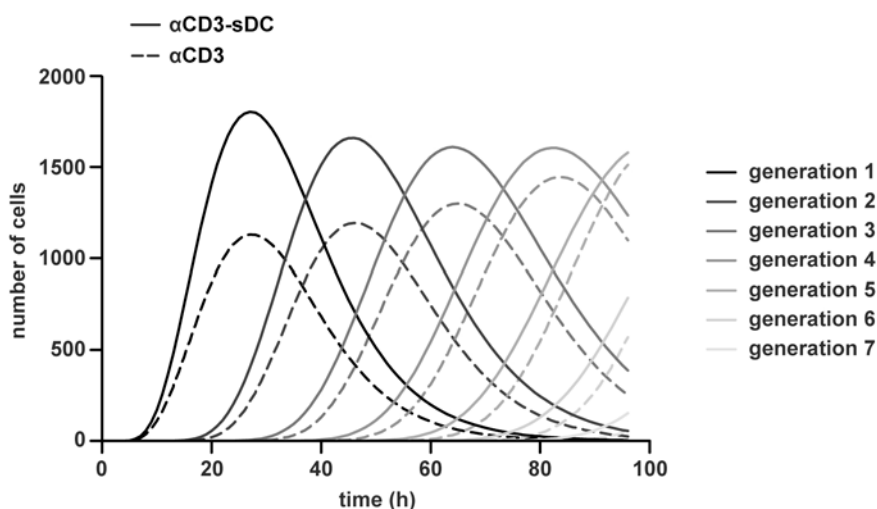


Figure S8. T cell proliferation determined with a CFSE assay. The graph represents the increase in the number of T cells per generation after treatment with α CD3-sDC and soluble α CD3, respectively. In the case of the α CD3-sDC treatment, the cell proliferation rate increases to a maximum in the first generation. This proliferation rate was maintained over the following generations (for the complete time period analyzed). When treating the T cells with soluble α CD3, the cell number only gradually increases per generation.

10. Statistical analysis

Two-way ANOVA and Bonferroni post-tests were performed for a pair wise comparison between the variables using Graphpad Prism 5 software (San Diego, CA, USA). The statistical significance is defined as $p < 0.05$. The asterisk ‘*’, ‘**’, ‘***’ represents p values <0.05 , <0.01 and <0.001

11. Confocal imaging

The binding of α CD3-sDC on the T cell surface was analyzed by confocal imaging using sDCs carrying a fluorescein-labelled α CD3 antibody (F α CD3-sDC). PBLs (10^5 /well) were treated for 24 h with F α CD3-sDC and F α CD3 (F-Fluorescein, $\lambda_{\text{ex}} = 488$ nm, $\lambda_{\text{em}} = 520$ nm) at different concentrations (5, 10, 20, 30, 50, 200 ng/mL). Further, these cells were labelled with the membrane dye PKH26 ($\lambda_{\text{ex}} = 551$ nm, $\lambda_{\text{em}} = 567$ nm; Sigma Aldrich) following the manufacturer's protocol. These labelled PBLs were fixed in 4 % paraformaldehyde. The fixed cells were quenched with glycine (0.1 mM) in PBS. The cover slips were mounted onto microscope slides (Thermo Fisher Scientific) using MOWIOL (Merck Millipore). The slides were imaged using a Confocal Laser Scanning Microscope (Olympus FV1000) equipped with a 63x oil immersion objective.

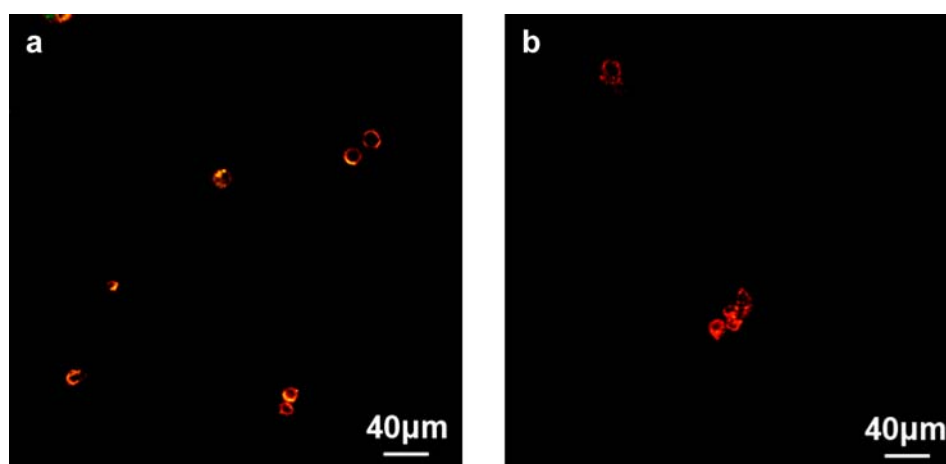


Figure S9. Overview images illustrating co-localization (yellow) of (a) Fluorescein-labelled α CD3 (F α CD3, green) loaded onto polymer **6** (F α CD3-sDCs) and (b) free F α CD3 on the PBL membrane (stained with the membrane specific dye PKH26, red).

The cells that show bound F α CD3-sDC were counted manually and compared to the number of F α CD3-sDC-free cells (Figure S9) using the program ImageJ. All the

experiments were repeated three independent times using PBLs from three different healthy donors.

12. Comparison of α CD3-sDC efficacy with α CD3-PLGA particles

12.1. Synthesis of α CD3-PLGA particles

A particle based DC system was prepared using PLGA particles as described previously¹⁰ with the following modifications. To attach the α CD3 antibody to PLGA via the SA_v-biotin interaction, SA_v was covalently coupled to the PLGA particles (PLGA-SA_v). In brief, protected sulfhydryl groups were introduced into SA_v using N-Succinimidyl S-Acetylthiopropionate (SATP; Thermo Scientific) and deprotected with hydroxylamine hydrochloride (Thermo Scientific) using the manufacturer's protocol. Thereafter, the free thiol-groups on the SA_v were reacted with the maleimide group of the DSPE-PEG-maleimide (MW = 2000 g/mol) that is present on the PLGA surface. After washing with PBS, the biotinylated α CD3 antibody was bound to PLGA-SA_v to obtain α CD3-PLGA.

12.2. Characterization of α CD3-PLGA particles

The size and concentration of the SA_v-PLGA and α CD3-PLGA were determined using Transmission Electron Microscopy (TEM; JEOL TEM 1010, Nieuw-Vennep, The Netherlands) (Figures S10a and S10b) and Differential Interference Contrast (DIC; Figure S10c) using a confocal microscope (FluoView FV1000, Olympus, Zoeterwoude, The Netherlands).

To obtain the particle concentration, the particle suspension was imaged using a Bürker chamber. The suspension was imaged under semi-dry conditions on the Bürker chamber grid to ensure that all particles had settled on the grid surface. The number of particles

on the square grid was counted using the program ImageJ. For the α CD3-PLGA particles, the concentration was calculated to be $1.24 \cdot 10^{17}$ particles per mL. To estimate the amount of α CD3 bound per α CD3-PLGA particle, a biotinylated and AlexaFluor488-labelled α CD3 antibody was used in the same way as described for the α CD3-sDCs described above (see 6.). This experiment yielded an amount of 3795 α CD3 antibodies per PLGA particle. For the T cell experiments, where no fluorescently labelled antibody was used, it has been assumed that the amount of bound α CD3 will be the same for identical experimental conditions.

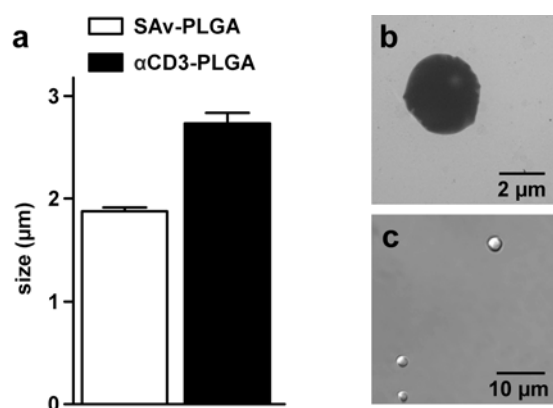


Figure S10. Characterization of α CD3-PLGA particles. a) Particle size obtained from TEM. The result represents mean \pm s.e.m. ($n = 300$ particles); b) representative TEM image of α CD3-PLGA; c) representative DIC image of α CD3-PLGA.

12.3. Estimation of the contact area and the number of possible interactions

Based on the above measurements the surface density of α CD3 antibodies on the PLGA particles can be calculated. The average number of 3795 α CD3 molecules per PLGA particle corresponds to 1 α CD3 antibody within 2688 nm^2 and an average distance between antibodies of roughly 50 nm. This in turn allows us to obtain the number of possible interactions with the cell surface.

Before this number can be calculated, the contact area of the PLGA particle with the cell has to be determined first. The calculation of the contact area is based on Hertz theory:¹¹

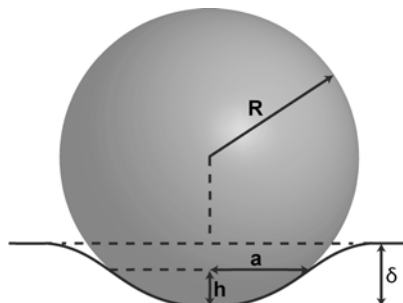


Figure S11. Geometry of the particle membrane interaction; with R - particle radius, δ - indentation depth, a - radius of the contact area.

The contact area A is described by $A = 2\pi R h = 2\pi R^2 \left(1 - \sqrt{1 - \frac{a^2}{R^2}}\right)$ (1)

with $a^2 = R\delta$.

To obtain the contact area, first the force F that the particle exerts on the cell surface and the corresponding indentation depth δ are calculated:

The indentation depth δ and the Force F are related by the following equations:

$$F = \frac{4}{3} E^* R^{\frac{1}{2}} \delta^{\frac{3}{2}} \quad (2)$$

and

$$\delta = \left(\frac{3}{4} \frac{F}{E^*}\right)^{\frac{2}{3}} \cdot R^{-\frac{1}{3}} \quad (3)$$

with the combined elastic modulus $\frac{1}{E^*} = \frac{1 - \nu_{cell}^2}{E_{cell}} + \frac{1 - \nu_{particle}^2}{E_{particle}}$ (4)

First, we estimate the force as a function of gravity to model the natural “bouncing” of the sphere into the cell membrane in an aqueous environment. A radius of $R = 0.9 \mu\text{M}$

has been determined for the SAV-PLGA particles (Figure S9). These particles have a density that is 1.2x larger than the density of water. Using equation (5)¹² the maximum speed v_a that a PLGA particle can reach in an aqueous environment can be calculated:

$$v_a = \frac{2R^2\Delta D_r g}{9\eta} \quad (5)$$

with ΔD_r - difference in density, g – gravitational acceleration, η – viscosity of water

For the PLGA particles we find:

$$v_a = 0.353 \text{ } \mu\text{m/s}$$

The corresponding force can then be calculated for low Reynolds number ($Re \ll 1$):

$$F = f \cdot v \quad (6)$$

where f depends on the particle radius R and the viscosity of the environment η via

$$f = 6\pi\eta R \quad (7)$$

In this way the force exerted by the particle on a cell can be estimated as

$$F = 6 \cdot 10^{-15} \text{ N for } v = v_a$$

Cells are known to have a Young's Modulus of $\approx 400 \text{ Pa} - 2500 \text{ Pa}$,¹³ which is much smaller than that of PLGA particles. Therefore, E^* can be simplified as:

$$\frac{1}{E^*} = \frac{1 - \nu_{cell}^2}{E_{cell}} + \frac{1 - \nu_{particle}^2}{E_{particle}} \approx \frac{1 - \nu_{cell}^2}{E_{cell}} \quad (8)$$

Using equations (1) – (8), a PLGA particle consequently indents a cell by $\delta = 0.16 \text{ nm}$.

The corresponding contact area between the cell and the PLGA particle is $A = 450 \text{ nm}^2$ meaning that the PLGA particle interacts with the cell over a distance of roughly 25 nm.

Without the 20 nm PEG spacers used for antibody attachment maximally 1 or 2 antibodies could interact with the cell at the same time. Considering the flexible spacers, up to 10 antibodies are able to interact with the cell simultaneously. Based on these

results it can be concluded that multivalent interactions can also take place when using α CD3-PLGA particles. More importantly, the total number of antibodies able to interact with the cell and the spacing between them is nearly the same for both the α CD3-PLGA particles and the α CD3-sDCs (approx. 50 nm in both cases).

References

1. P. H. J. Kouwer, M. Koepf, V. A. A. Le Sage, M. Jaspers, A. M. van Buul, Z. H. Eksteen-Akeroyd, T. Woltinge, E. Schwartz, H. J. Kitto, R. Hoogenboom, S. J. Picken, R. J. M. Nolte, E. Mendes and A. E. Rowan, *Nature*, 2013, **493**, 651-655.
2. M. Koepf, H. J. Kitto, E. Schwartz, P. H. J. Kouwer, R. J. M. Nolte and A. E. Rowan, *Eur. Polym. J.*, 2013, doi: 10.1016/j.eurpolymj.2013.01.009.
3. I. Teraoka, *Polymer Solutions: An Introduction to Physical Properties*, John Wiley & Sons, New York, 2002.
4. A. J. M. van Beijnen, R. J. M. Nolte, W. Drenth, A. M. F. Hezemans and P. J. F. M. Vandecoolwijk, *Macromolecules*, 1980, **13**, 1386-1391.
5. C. A. Schneider, W. S. Rasband and K. W. Eliceiri, *Nat. Methods*, 2012, **9**, 671-675.
6. R. Supino, in *In Vitro Toxicity Testing Protocols*, eds. S. O'Hare and C. K. Atterwill, Humana Press, Totowa (NJ), 1995, pp. 137-149.
7. R. I. Freshney, in *Culture of Animal Cells: A Manual of Basic Techniques*, ed. R. I. Freshney, Alan R. Liss New York, 2000, p. 173.
8. A. D. Wells, H. Gudmundsdottir and L. A. Turka, *J. Clin. Invest.*, 1997, **100**, 3173-3183.

9. E. D. Hawkins, M. Hommel, M. L. Turner, F. L. Battye, J. F. Markham and P. D. Hodgkin, *Nat. Protoc.*, 2007, **2**, 2057-2067.
10. L. J. Cruza, P. J. Tacken, R. Fokkink, B. Joosten, M. C. Stuart, F. Albericio, R. Torensma and F. C. G., *J. Controlled Release*, 2010, **144**, 118-126.
11. V. L. Popov, *Contact Mechanics and Friction: Physical Principles and Applications*, Springer, Berlin, 2010.
12. J. Newman, *Physics of the Life Sciences*, Springer, New York, 2008.
13. Y. Shimizu, T. Kihara, S. M. A. Haghparast, S. Yuba and J. Miyake, *PLoS ONE*, 2012, **7**, e34305.